ELSEVIER

Materials Science and Engineering A 487 (2008) 235–242

MATERIALS SCIENCE & ENGINEERING A

www.elsevier.com/locate/msea

Effect of fibrous orientation on dynamic mechanical properties and susceptibility to adiabatic shear band of tungsten heavy alloy fabricated through hot-hydrostatic extrusion

Liu Jinxu, Li Shukui *, Fan Ailing, Sun Hongchan

School of Materials Science and Engineering, Beijing Institute of Technology, Beijing 100081, People's Republic of China

Received 18 April 2007; received in revised form 3 October 2007; accepted 3 October 2007

Abstract

The tungsten heavy alloys (WHAs) with fibrous grains were obtained by hot-hydrostatic extrusion at 950 °C with plastic deformation ratio of 75%. Dynamic mechanical behaviors under uniaxial dynamic compression were systematically investigated with the angles between the loading direction and the extruding direction being 0°, 45° and 90°. The testing results show obvious difference in dynamic behaviors and susceptibility to adiabatic shear band (ASB) for different specimens. In the 0° specimens, no localized flow is observed. The 45° specimens exhibit slight localized shearing. In the 90° specimens, localized ASB was firstly observed at an angle of 45° with respect to the fibrous orientation followed by cracking, which is greatly desirable for kinetic energy penetration applications. Microstructure analyses reveal that the high susceptibility to ASB of the 90° specimens result from adiabatic temperature rising during dynamic loading and reduced strain hardening caused by the special micro-strained condition and fiber distribution.
© 2007 Elsevier B.V. All rights reserved.

Keywords: Tungsten heavy alloy; Adiabatic shear band; Dynamic mechanical behavior; Hot-hydrostatic extrusion; Fibrous orientation

1. Introduction

Tungsten heavy alloys (WHA) are usually fabricated by powder metallurgy method. Typical structure of WHA is that BCC tungsten particles are uniformly distributed on ductile FCC matrix. WHA are wildly used in many applications such as kinetic energy penetrators, radiation shields and counter weights due to their high density (16–18.5 g/cm^3) and excellent mechanical properties [1].

Penetration performance of kinetic long rods is mainly dependent on two factors of materials when the shape of penetrators is fixed. One factor is excellent mechanical properties of materials including high strength, good toughness and ductility which ensure materials used for penetrator surviving the severe their launch and touchdown. The other factor is high "self-sharpening" capacity of materials which makes materials fall off timely along the adiabatic shear band (ASB) during the penetrating process [2]. The abrupt concentration of heat converted from the large plastic deformation in several μs during penetration is favorable for ASB. Subsequently, along the ASB, the crack usually appears at the edges of the penetrator head and therefore reduces the diameter of the penetration tunnel [3]. Unfortunately, WHAs is well known to be resistant to adiabatic shear banding because of their strong rate sensitivity, and the kinetic energy penetrators made of WHAs usually form mushroom-like head which results in poorer penetration performance than depleted uranium alloys (DU). The better penetration performance of DU can be attributed to their good susceptibility to ASB. However, application of DU has raised serious, long-term environmental and health concerns. Shear localization in WHAs has been sought for many years, and a large amount of work on alloying [4,5], strain hardening [6], heat treatment [7], and microstructure refinement by solid sintering [8] has been done to improve susceptibility to ASB of WHAs for the application of penetrators with prominent self-sharpening capacity. However, such efforts have met with little success, despite the wide range of alloying elements that have been introduced to tailor the phase composition and microstructure.

In the past, flow localization in WHA and pure W has often been induced by intentionally generating localized shear stresses

* Corresponding author. Tel.: +86 13701219671; fax: +86 01068913951x88.
E-mail address: bitleesk@bit.edu.cn (S. Li).

0921-5093/$ – see front matter © 2007 Elsevier B.V. All rights reserved.
doi:10.1016/j.msea.2007.10.012

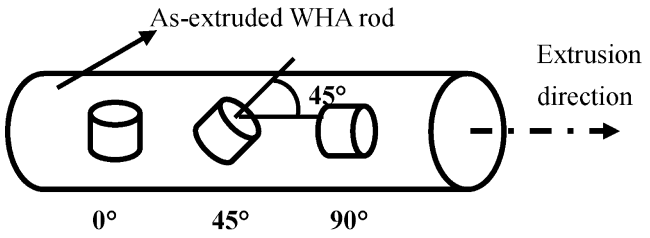

Fig. 1. Schematic of the 0°, 45° and 90° specimens machined off the as-extruded WHA rod.

in the specimen through special design of specimen geometry [9]. In the recent work of Q. Wei et al. [10–12], both nanocrystalline tungsten fabricated by high-pressure torsion (HPT) and ultrafine grained tungsten obtained by rolling after equal channel angular pressing (ECAP) exhibit localized shearing under uniaxial dynamic compressive loading. But so far, no flow localization has been reported to be observed in bulk WHA under uniaxial dynamic compression.

In this paper, hot-hydrostatic extrusion was applied to liquid-phase sintered WHA in order to obtain fibrous microstructure. The purpose is to explore the possibility of improving susceptibility of WHAs to ASB. Dynamic failure mechanisms and susceptibility to ASB under uniaxial dynamic compression of the as-extruded WHA along different fibrous orientation were systematically investigated.

2. Experimental

Initial materials investigated in the present study are liquid-phase sintered 94.9W–3.4Ni–1.6Fe–0.1Co. The as-sintered 94.9W–3.4Ni–1.6Fe–0.1Co was further processed by hot-hydrostatic extrusion at 950 °C with a plastic deformation ratio of 75%. Both the as-sintered and as-extruded WHA specimens were sectioned longitudinally and transversely for metallographic examination. Cylindrical specimens (Φ5 mm × 5 mm) for uniaxial dynamic compression testing were machined off the as-extruded WHA rods by electro-discharge machining (EDM), with the angles between the cylinder axial direction and the extruding direction being 0°, 45° and 90°, as shown in Fig. 1. For convenience, the three kinds of specimens were referred to as the 0° specimen, the 45° specimen and the 90° specimen, respectively. Uniaxial dynamic compression tests were carried out using Split Hopkinson Pressure Bar (SHPB) at an average strain rate of about 3000 s^{-1}. The fracture surfaces of the tested specimens were examined by scanning electron microscopy (SEM) coupled with energy dispersive X-ray spectroscopy (EDX). The fractured 45° and 90° specimens were sectioned along the compressing axis as displayed in Fig. 2, and the sectioned surfaces were polished to a mirror finish in order to observe the localized flow and the fibrous orientation (the space position between fibrous orientation and fracture surface was revealed by observation of the fibrous orientation on the sectioned faces). The other specimens which had not been fractured under a lower projectile velocity were also sectioned along the compressing axis and the sectioned surfaces were polished in a similar way.

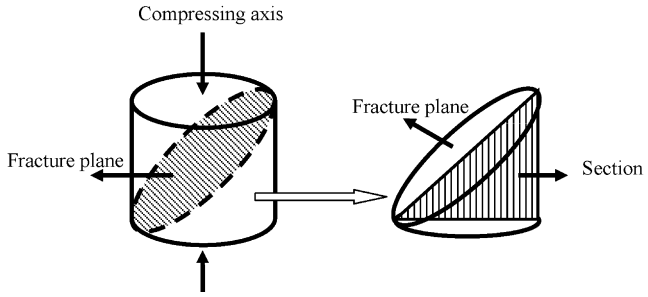

Fig. 2. Schematic of sectioning the fractured 45° and 90° specimens for metallography examination.

3. Results

3.1. Microstructures

Tungsten grains and matrix are heavily deformed by hot-hydrostatic extrusion. Fig. 3(a) displays the microstructure of as-sintered 94.9W–3.4Ni–1.6Fe–0.1Co alloy with spherical tungsten grains distributed uniformly on the matrix. Fig. 3(b) and (c) shows microstructures on the longitudinal and transverse sections of as-extruded 94.9W–3.4Ni–1.6Fe–0.1Co alloy. It can be observed that tungsten grains were elongated into fibrous shape, and the average aspect ratio is about 10.

3.2. Dynamic mechanical properties and susceptibility to ASB

The dynamic mechanical behaviors of the three typical of specimens (0°, 45° and 90°) were performed by using Split Hopkinson Pressure Bar (SHPB) at an average strain rate of 3000 s^{-1}, and the as-sinter WHA was also tested for comparison. Fig. 4 displays images of the specimens before and after uniaxial dynamic compression. The 0°, 45° and 90° have obviously different failure modes under dynamic compression. The 0° and the as-sintered specimens exhibit considerable uniform plastic deformation without fracture, indicating good dynamic compressive ductility. When the velocity of the projectile is increased in uniaxial dynamic compression, the 0° specimens fractured along the plane which is parallel to compressing axis. Fig. 4 also displays the fractured 45° and 90° specimens. Clearly, the failure occurred on the plane of maximum shear stress (PMSS). It can be observed from Fig. 4 that the 45° specimens have experienced slightly more severe plastic deformation than that of the 90° specimens.

Fig. 5 shows the uniaxial dynamic compressive true stress–strain curves of the 0°, 45°, 90° and as-sintered specimens. The 45° and 90° specimens shows a peat flow stress as high as 2350 MPa, but the peat flow strength of the 0° specimens is lower than 2350 MPa, though it is still much higher than 1500 MPa of the as-sintered specimens. From the curves in Fig. 5, the critical strain for fracture of the 90° specimens (0.15) is half the value of the 45° specimens (0.3). We should point out that the final load drop of the 0° and as-sintered specimens are due to unloading at a prescribed strain level. Another important observation from these true stress–strain curves is the clear stress

Download English Version:

https://daneshyari.com/en/article/1582565

Download Persian Version:

https://daneshyari.com/article/1582565

Daneshyari.com